Active Magnetic Bearing Positioning in the Conceptual Design Phase of a High-Speed Electric Machine

Emil Kurvinen, Juuso Narsakka, Tuhin Choudhury, Rafal P. Jastrzebski *Member, IEEE*, Jussi Sopanen *Member, IEEE*

***Abstract*—The optimization of high-speed active magnetic bearing rotor layout concerning the effect of external disturbance is studied. The centrifugal loads and related strain forces in the HS rotors limit the maximum rotational speed and AMB capacity, bandwidth, and location limit control of dynamics. Additionally, external synchronous disturbances, *i.e.*, unbalance forces, rotor runout, application forces from the impeller, and static forces cause adverse effects on active control and pose limitations. Therefore, to achieve a sub-critical rotor, the dimensions of electric machine components, such as bearings, seals, and impellers affect each other and have to be constrained. The proposed method examines the effect of disturbances and locations and resulting dynamic limitations at the conceptual design phase. This enables the design of the AMBs and component layout to the application demands. The method uses maximum singular values to examine the effects of disturbances on bearing forces and rotor displacements at key locations.**

***Index Terms*—High-Speed, Rotordynamics, Electric Machine, Active Magnetic Bearing**

NOMENCLATURE

$\bar{z}$	Normalized output quantities
d_{amb}	AMB diameter (mm)
d_{em}	Active part diameter (mm)
d_{end}	Rotor end diameter (mm)
d_{s1}	Section 1 diameter (mm)
d_{s2}	Section 2 diameter (mm)
F_{amb}	AMB load capacity (N)
G_{yu}	y and u components of transfer-function matrix
G_{yw}	y and w components of transfer-function matrix
G_{zu}	z and u components of transfer-function matrix
G_{zw}	z and w components of transfer-function matrix
l_{end}	Rotor end length (mm)
l_{s1}	Section 1 length (mm)
l_{s2}	Section 2 length (mm)
u	System input
w	Disturbance force (N)
w_1	Disturbance force to impeller
y	System output
z	Performance output constraints (mm and N)
z_{DDE}	Drive end sensor displacement (mm)
z_{DNDE}	Non-drive end sensor displacement (mm)
z_{FDE}	Drive end bearing force capacity (N)
z_{FNDE}	Non-drive end bearing force capacity (N)
z_{IMP}	Impeller displacement (mm)

Prof. E. Kurvinen, corresponding author, is with Materials and Mechanical Engineering University of Oulu, Pentti Kaiteran katu 1, 90570 Oulu, Finland, Emil.Kurvinen@oulu.fi

J. Narsakka, T. Choudhury, Prof. J. Sopanen are with Department of Mechanical Engineering, Lappeenranta-Lahti University of Technology LUT, Yliopistonkatu 34, 53850 Lappeenranta, Finland, Juuso.Narsakka@lut.fi & Tuhin.Choudhury@lut.fi & Jussi.Sopanen@lut.fi

R. P. Jastrzebski is with Department of Electrical Engineering, Lappeenranta-Lahti University of Technology LUT, Yliopistonkatu 34, 53850 Lappeenranta, Finland, Rafal.Jastrzebski@lut.fi

I. INTRODUCTION

HIGH-SPEED electric machines enables to achieve high efficiency and high power density, *i.e.*, compact structure. This is especially desirable in the industry when the sustainability and carbon footprint over the lifecycle of the product are focused, *e.g.*, by using fossil-free steel or green steel [1], [2]. Often advanced bearing technologies are also involved, as they give the capacity to influence the performance during operation, such as with active magnetic bearings (AMBs). Also rolling element bearings (REBs) and journal bearings are utilized, but they have limited capacity for active control. AMBs are commonly used in the high-speed and high-power machines (hundreds of kilowatt to megawatt range), where the losses of REBs are high and the remaining useful lifetime (RUL) is related highly to the loads experienced during the lifecycle. In this study, the focus is on AMBs as those have by nature the possibility to influence the dynamic behavior of the system, *i.e.* enabling active influence and vibration dissipation strategies. As the AMBs are actively controlled, they require high sampling information of the rotor position with respect to the stationary part, which requires a displacement sensor. [3] Typically in the integrated solution, the rotor is supported with two radial AMBs and an axial bearing to withstand the load from the application, *e.g.*, compressor. Integrating the application directly to the machine is attractive, as the whole construction can be made very compact and avoid additional components such as gearbox and extra bearings, *e.g.*, due rotating standalone compressor. The drawback of a highly integrated solution is its lack of modularity, a requirement of highly skilled persons to optimize the operation and *e.g.*, adjusting the AMB's performance at the operation and higher power rates at the manufacturing. [4], [5] To improve the scalability and

modularity, multiple bearings are proposed in the integrated machine structure to accommodate the design for different applications. [6]

The control of the AMBs in the industry still relies on the traditional PID controller and is widely applied in industrial applications due to its robustness and performance, even though the scientific community proposes several developments by applying advanced controls for improved performance. [7]

The design and manufacturing of integrated solutions require work and at high power rates, the manufacturability becomes challenging, especially the rotor part, which is operating near the physical limits. [5] For better modularity a detailed understanding of the design limitations is important to understand, *i.e.* the pros and cons of design changes to the system performance (disturbance forces, physical movement of the rotor). In the conceptual design phase, the computational methods are used, and verified practices are used to assess the system performance. This can be further utilized when assessing the limits of each design, as shown in Kurvinen et al. [8]. The fundamental limits arise from the length of the rotor and the rotation speed of the rotor. The larger diameter means higher stresses, and therefore requires high-strength materials to cope with the higher loads. The length of the rotor is related to the rotation speed, *i.e.*, the long rotor goes to resonance at a lower speed compared to the shorter rotor. The industry trend is going for higher power applications, *e.g.*, as reported in Moghaddam, most of the machines were below 1000 kW [9] and recent examples in megawatt size have been published [8], [10] with the integrated solutions. To achieve higher power and increased speed the challenges to handle higher stresses and yet keep the dynamical performance acceptable, *i.e.* avoiding resonances creates design challenges.

The dimensioning and positioning of the AMB affect the performance of the system. The AMBs are typically dimensioned based on the static load, *i.e.* structure own weight, which they should be able to carry and multiplying that with a factor 4-7 [6], also the maximum pressure achievable with magnetic forces are limited [6]. The AMB dimensions (length and outer radius of the magnetic bearings) are important parameters for achieving magnetic levitation. The dimensions are calculated based on the force specification along with a factor of safety for levitating the rotor under the dynamic loads during operation [11]. Similarly, the location of the AMB is also very significant. AMB utilizes feedback from position sensors to calculate the current and generate the required amount of force in the corresponding direction to keep the shaft at the center. To ensure this, the nodal location of the operational mode should not coincide with the location of either the sensors or the actuators. This is referred to as 'non-collocation' of the gap sensors, bearing actuators, and the nodal locations and it is an important checkpoint in AMB design [12].

Often the AMBs are identical both in the driven end and non-driven end. However, in the application of a compressor, the driven end experiences dynamical loads from the application, which gives higher requirements for the bearings to cope. In systematic engineering [13], the first step is to define the requirements, and the following step is to explore different conceptual designs. In electric machines, for the conceptual design and layout of the rotor, there is still space for more optimization of the system performance. In a typically integrated rotor, electric machines are producing the torque, bearings to support the structure, position measuring planes to input the position information for AMBs, backup bearings to guarantee the performance in the event of power outtake, and balancing planes to get the rotor balanced, seals to prevent leakages and achieving high efficiency to the system.

The nodal locations and vibration mode shapes are required to consider already in the design phase to avoid positioning the bearings and sensor locations directly on top of the nodal locations.In this case, the bearings or sensors can control the mode, as it cant be detected with sensors or actuated with the bearings. The rotor can be controlled in case the sensor is located on another side of the nodal location than the bearings, *i.e.* with non-collocation, where the phase difference is compensated in the control design. However, the position of the bearings and sensors has a great influence on the amount of authority that they have with respect to the vibration modes. Therefore the largest distance from the nodal location would be desirable to maximize the authority. In the study, the performance of the conceptual design phase rotor is assessed. The objective is to dimension the DE bearing and find the optimal locations for the bearings and sensors concerning the performance and authority to control vibration modes.

In the AMBs the bearings are designed for specific load capacity, *i.e.* loads that it should be able to support. In addition, there is air gap length between the rotational and stationary parts. As per standard definition, backup bearings are needed, and their airgap length is typically half of the total air gap length, *i.e.*, the rotor can move radially half of the airgap length before dropping to the backup bearings, which ensures that the operability of machine withstands in case of power malfunction or exceeding loads to the system. In the design phase of AMBs, the system sensitivity and capacity to handle additional load can be assessed with limiting load capability effectively with computationally efficient modeling methods for example as shown in Kurvinen et al. [4], where the additional radial force is induced in compressor application to the impeller.

The novelty of the present study is proposing a method for conceptual phase design to optimize the bearing size and its position in the rotor, in order to have the largest authority concerning the disturbance loads to the rotor. This enables to dimension and position of the AMBs in the conceptual design phase effectively.

II. Machine load capacity

Computational efficient physics-based simulation techniques are useful in the design phase, where a different combination of designs and related parameters are explored. When designing a high-speed electric machine rotor, Timoshenko beam element [14] based models are utilized in the conceptual design phase. The geometries are symmetrical around the rotational axis, and therefore the simple element type can represent the system and its dynamic behavior well. In addition, assessing the dynamical properties can be done with a low amount of elements to account for the dynamical properties accurately, and therefore the more coarse number of elements gives enough good criteria for understanding the dynamics.

To study input and output for a linear system the equation of motion can be presented in state-space form. It is widely used and applied in control engineering. [3] The dynamical model of a rotor system can be represented in state-space form when mass, stiffness, and damping matrices are known. In addition, information about nodal locations is needed to assess the input and output locations and their physical units.

Active magnetic bearing load capacity can be estimated by the physically possible electromagnetic force per area, *e.g.*, with traditional laminate material, 37 N/cm^2 and by multiplying the projected area, *i.e.* diameter of the bearing with the length of the bearing [6]. Therefore in the design phase, the basic value for the physically possible bearing force can be estimated. The controllability of the AMBs is related to bearing and sensor collocation with the vibration modes' nodal locations. In the control design phase, the non-collocation can be considered with the phase difference, however at nodal locations the detection or acting for a specific vibration mode is compromised. [3]
Machine load capacity based on singular value decomposition (SVD) method [15] is used similarly as was described in [4] for the objective of determining the physical limits in the conceptual design phase. This allows for justifying the sizing and locations of the bearings at the rotor.

The disturbance force (w) input is applied to the application end in the radial direction, *i.e.*, to the impeller, where, *e.g.*, the force due to the unbalance occurs during operation, for example from dirt accumulation or failures. The rotor construction is overhang type, and at the end of the rotor, the force has the biggest moment arm and therefore creates the largest disturbance effect. The load capacity is defined by the maximum allowed force that the performance output constraints (z) are not violated, *i.e.* the displacement constraint (at sensor locations and impeller location) and maximum force capacity that AMBs can produce. The rotordynamics calculation model is used to assess the load capacity by forming it in the state-space form and calculating the $\mathcal{H}_2$ norm optimization control calculation as shown in [4] and is here shortly described.

The normalized response of the system with respect to the disturbance input can be calculated as

$$\bar{z} = G_{zw}w + G_{zu}u \quad (1)$$

$$y = G_{yw}w + G_{yu}u \quad (2)$$

The maximum disturbance force is defined to be the largest force applied as input w that the normalized measured output quantities, $\bar{z}$, are less than one in magnitude. Appendix I depicts the used calculation algorithm loop.

Limiting performance is defined as the limiting disturbance force to the system that the output quantities are not exceeded while the AMB's physical properties and system dynamical behavior is guaranteed. In the study, the disturbance force is given in the frequency domain and the limiting output criteria is selected out of the quantities, *i.e.* which is the limiting factor at different frequencies. In the analysis, the controller performance is assumed to have infinite bandwidth, *i.e.* simplifying the analysis and also giving some limitations for the performance. For the design purpose, especially in the conceptual design phase, the overall relations between different parameters are important, and therefore the justification for omitting the control design is justified.

This is accomplished by replacing u with u^* (ideal) from Eq. (1) by calculating the two norm (eucledian norm) as [4]:

$$u^* = \arg\min_u |\bar{z}|_2 , \quad (3)$$

which enables to represent the system as:

$$|\bar{z}|_2^2 = w'G'_{zw}G_{zw}w + u'G'_{zu}G_{zu}u + 2u'G'_{zu}G_{zw}w \quad (4)$$

This produces the 2–normed optimal response to any given disturbance load w:

$$\bar{z} = \left[I - G_{zu}\left(G'_{zu}G_{zu}\right)^{-1}G'_{zu}\right]G_{zw}w \equiv H_o w \quad (5)$$

The largest possible induced 2–norm is then $\bar{\sigma}(H_o)$. Given the proxy objective to find the smallest w that produces $|\bar{z}|_2 = 1$, this means that the machine load capacity would be

$$w_{\max,2}(j\omega) = \frac{1}{\bar{\sigma}(H_o(j\omega))} \quad (6)$$

The 2-normed solution is representing the average bandwidth with respect to the frequency spectrum, whereas the infinity norm would enable to optimization of the performance to a specified frequency range, *i.e.* optimize the performance better at limited bandwidth. In addition, the analysis does not consider the amplification, sensor noise, or slew rate, which limits the actual achievable performance at higher frequencies. However, the analysis assesses the overall behavior and enables a comparison of different configuration effects on the system performance.

III. Case studies

In the study, the case studies are selected that represent typical high-speed and high-power electric machines. The varied geometries thereby are extrapolated from the realistic machine. A basic model shown is described in the following section, which is modified by shifting the drive-end AMB

closer to the impeller while keeping the total length fixed. Three different cases are evaluated and their effect on the capacity to handle disturbance loads and nodal locations are studied to estimate the feasibility and performance capability of the different rotors.

A. Rotor models

A finite element method (Timoshenko beam elements) was used to develop the model of the flexible rotor. The solid steel rotor was modeled with 27 Timoshenko beam elements. The impeller, bearing and motor laminations, and thrust disk was modeled as lumped mass elements, *e.g.*, they were assumed not to produce additional stiffness to the rotor. The model was used to produce the rotor state-space model and calculate the free-free modes and frequencies.

In the study, a baseline model rotor from [8] is used. Figure 1a depicts the rotor model with the performance criterias, z and disturbance load w_1 and Fig. 1b the rotor layout. Table I depicts the rotor parameters.

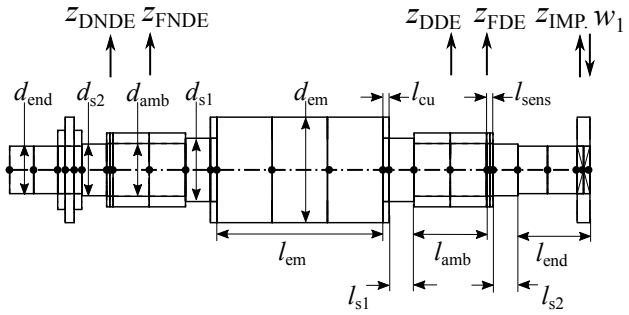

(a)

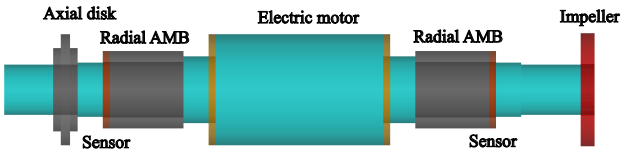

(b)

Fig. 1. (a) Rotor main dimensions and inputs and outputs (b) Layout of the rotor with main components

A state-space model is created of the rotor, where the inputs and outputs are defined as shown in Fig. 1, *i.e.* five outputs, three displacements (z_{DNDE}, z_{DDE} and z_{IMP}) corresponding non-drive end sensor displacement, drive end sensor displacement and impeller displacement and two forces z_{FNDE} and z_{FDE}, corresponding non-drive and drive end bearing force capacities. These outputs represent the actual rotor boundary conditions for the physical limitations. The system disturbance load is applied into impeller location in radial direction, w_1. This could be due to unbalance e.g. dirt

TABLE I
BASELINE DIMENSIONS CALCULATED ANALYTICALLY FROM DESIGN FROM DESIGN REQUIREMENTS

Parameters	Case 1 [8]	Case 2	Case 3
Rotordynamic Parameters			
Rotor mass (kg)	75.3	76.0	76.3
1st free-free frequency (Hz)	651.6	665.4	668.3
2nd free-free frequency (Hz)	1197	1225	1237
Active area from slit stress (Mech)			
Active part diameter(mm), d_{em}	164.8	164.8	164.8
Slit max depth (mm)	41.0	41.0	41.0
Slit depth ratio	0.5	0.5	0.5
Nominal stress in tooth (MPa)	88.7	88.7	88.7
Number of slit	38.0	38.0	38.0
Slit width (mm)	2.5	2.5	2.5
Surface velocity (m/s)	130.4	130.4	130.4
Active area from Tangential Stress (EM)			
Tangential stress from EM Force (Pa)	21496.1	21496.1	21496.1
Active part length (mm) l_{em}	243.0	243.0	243.0
AMB section			
Diameter of AMB (mm), d_{amb}	82.4	82.4	82.4
Length of AMB (mm), l_{amb}	106.7	106.7	106.7
AMB load capacity (N) (37 N/cm^2), F_{amb}	3253	3253	3253
Rotor end shaft and back up bearing section			
Diameter (mm), d_{end}	74.2	74.2	74.2
Length (mm), l_{end}	106.1	96.1*	86.1*
General sections			
Section 1 Diameter (mm), d_{s1}	98.9	98.9	98.9
Section 1 Length (mm), l_{s1}	36.5	66.5*	76.5*
Section 2 Diameter (mm), d_{s2}	80.7	80.7	80.7
Section 2 Length (mm), l_{s2}	36.5	16.5*	16.5*

*) DE side length, NDE side similar as in Case 1

accumulation in the compressor impeller. In the analysis, 0.25 mm limit for displacements and 3253 N for force are given, which comes from the physical limitations.

In the case study three different configurations (Table I) are explored and their consequently ability to withstand disturbance force are evaluated.

1) Case 1 is as shown in [8].
2) Case 2 the DE l_{s1} is 30 mm longer, l_{s2} 20 mm shorter and l_{end} 10 mm shorter, *i.e.* shifting the DE AMB consequently 30 mm closer to impeller, while total length stays the same.
3) Case 3 the bearing is further shifted 10 mm closer to impeller by making DE l_{s1} 40 mm longer, l_{s2} 20 mm shorter and l_{end} 20 mm shorter compared to the Case 1.

B. Results of load capacity calculation

In the study, the frequency range from 0 to 250 Hz is investigated. In higher frequencies, the control system limitations come significant, e.g. slew rate. Figure 2 depicts the maximum disturbance load w_1 before violating the set displacement and force limits. The close-up depicts the influence of bearing position and its effect on the static load capacity. The static load capacity varies from 2255 N to 2510 N, depending on the case.

Figure 3a depicts the normalized limiting factors of displacements in the three different cases. It can be seen that the limiting displacement is the allowed displacement in the impeller section.

Figure 3b depicts the normalized limiting factors of AMB's load capacity. It can be seen that the DE AMB is

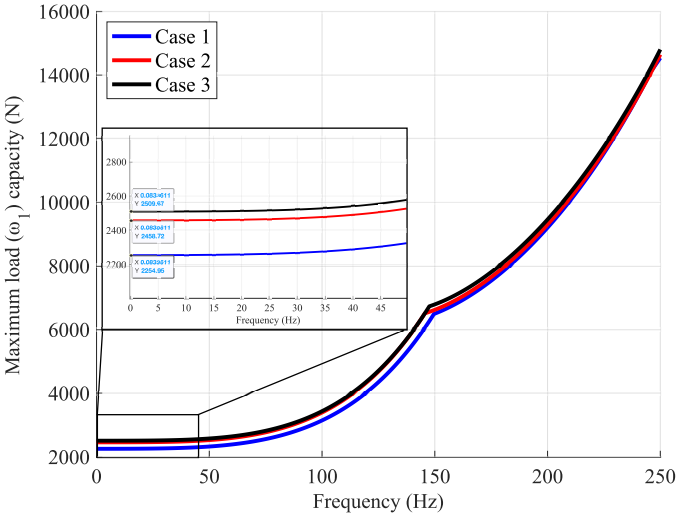

Fig. 2. Normalized system responses. Allowed maximum impeller forces at $\omega \in (0, 250)$ Hz

limiting the performance up to 150 Hz, *i.e.* by increasing the DE AMB size, it could perform better concerning the disturbance load. Also, it should be noted that NDE bearing is using half of its maximum capacity to withstand the disturbance load, *i.e.* its size could be minimized.

Figure 4 depicts the FE-model nodal locations and the first three bending modeshapes overlayed with the geometry.

The change of AMB location is also related to the flexible vibration modes nodal locations. In order to detect the vibration modes the nodal locations and collocation with sensor or actuator location should be avoided. Figure 4 depicts the three first bending modes and the FE-model related nodes.

Table II depicts the nodal locations of sensors and bearings and the distance to the closest nodal location and corresponding vibration mode.

IV. Discussion

In the study, the location of radial AMB and its sensitivity to output performance was assessed. The positioning is sensitive to the achievable disturbance loads. For example, static maximum disturbance load was from 2254 N to 2510 N when the AMB position was changed 5 cm in an 85.44 cm rotor. The calculation methodology omits the sensors and those dynamic effects, which would be used in the feedback loop of the actual system. The analysis method assumes an ideal situation, where all the system states are perfectly known, *i.e.* optimistic measurements. This means that an actual feedback-controlled system load capacity is expected to be less than the shown in the calculations, depending on the desired performance bandwidth. However, it shows the theoretical limitation, which can be used to estimate the final design expected performance limits. In high-speed machines the design is highly iterative and requires a feasible initial design to converge final design, thereby the rapid iterations and early design choices for the final product are important to consider.

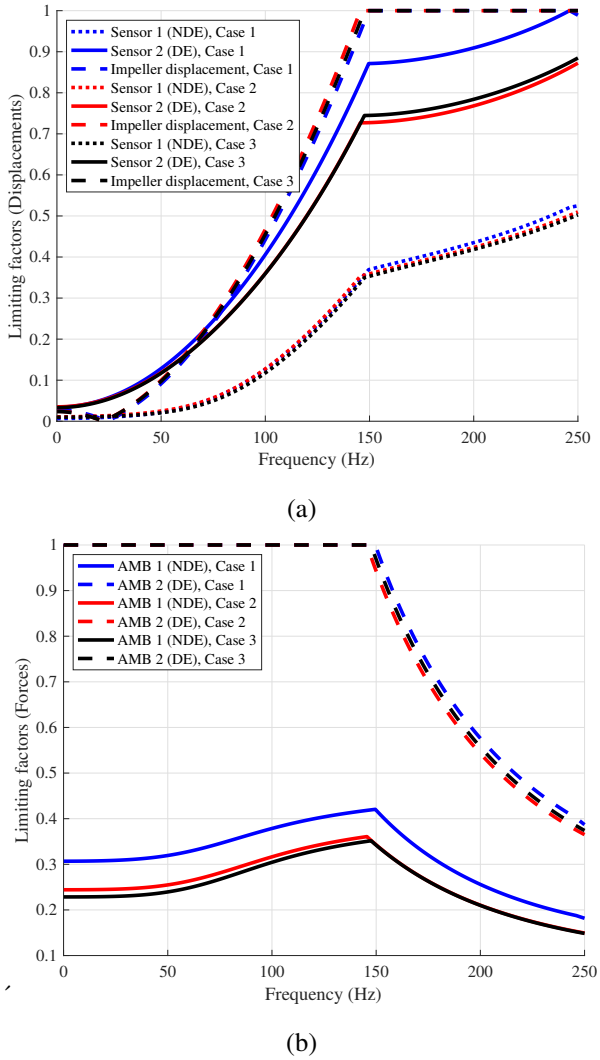

Fig. 3. Maximum singular values of the idealized closed-loop responses at respective locations to unbalance force from the impeller. At the AMBs the forces are measured; while at the sensor and impeller locations positions are measured. (a) Displacements as limiting factors (b) Forces as limiting factors

Dynamics and bandwidth limitations of the actuator can be included in the plant model with the inner current control loop approximated with the low pass filter, for example as in [6]. The proposed methodology allows studying different application options and situations, *e.g.*, different speeds, and performance capability with different weight impellers. Also, it can be used for sensitivity study to identify the parameters and their relation to other parameters, similarly as shown in [8].

V. Conclusions

In the study, the method for assessing the radial AMBs location and size in the conceptual design phase was developed. A case study with three variations was shown and the performance was assessed and compared. By this, the controllability of the bearings and authority for flexible

TABLE II
NODAL LOCATIONS AND CLOSEST BENDING MODES (FIRST THREE EVALUATED) NODAL LOCATIONS

		Case 1		Case 2		Case 3	
	Location [m]	Distance [m]	Modeshape	Distance [m]	Modeshape	Distance [m]	Modeshape
Sensor 1 (NDE)	0.1476	0.0088	2nd bending	0.0110	2nd bending	0.0119	2nd bending
AMB 1 (NDE)	0.2059	-0.0149	1st bending	-0.0114	1st bending	-0.0106	1st bending
AMB 2 (DE)	0.6485	-0.0278	1st bending	-0.0274	1st bending	-0.0270	1st bending
Sensor 2 (DE)	0.7069/0.6302	-0.0609	2nd bending	0.0369	3rd bending	-0.0453	1st bending

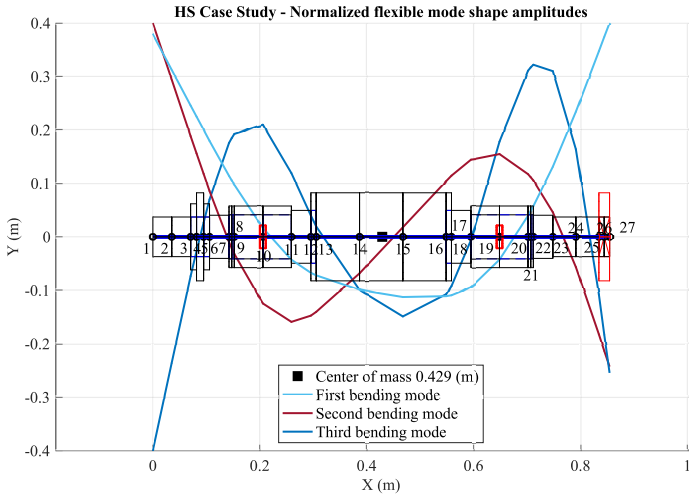

Fig. 4. Modeshapes and their nodal locations. Nodes 8 and 21 are sensors (NDE and DE) and 10 and 19 the AMBs (NDE and DE)

modes can be maximized while the sizing of the bearings can be optimized. The method is especially important in cases, where more than two bearings are utilized and the rotor is coupled with the application or additional rotor, where the flexibility of the rotor should be well known. The method enables to the assessment of the controllability and flexible modes of nodal locations in the early stage of the design. For future studies the modularity of design should be studied, *i.e.* what size of application or rotation speeds the given designs can handle with different applications. In addition the optimization of bearing sizes with respect to the disturbance loads. In a detail design, the closed-loop performance should be assessed.

REFERENCES

[1] M. Pei, M. Petäjäniemi, A. Regnell, and O. Wijk, "Toward a fossil free future with hybrit: Development of iron and steelmaking technology in sweden and finland," *Metals*, vol. 10, no. 7, p. 972, 2020.

[2] H. Muslemani, X. Liang, K. Kaesehage, F. Ascui, and J. Wilson, "Opportunities and challenges for decarbonizing steel production by creating markets for 'green steel'products," *Journal of Cleaner Production*, vol. 315, p. 128127, 2021.

[3] H. Bleuler, M. Cole, P. Keogh, R. Larsonneur, E. Maslen, Y. Okada, G. Schweitzer, A. Traxler, G. Schweitzer, E. H. Maslen *et al.*, *Magnetic Bearings: Theory, Design, and Application to Rotating Machinery*, 1st ed. Berlin Heidelberg: Springer Science & Business Media, 2009.

[4] E. Kurvinen, R. Fittro, and E. Maslen, "Improving compressor surge performance with advanced control," *Proceedings of the Institution of Mechanical Engineers, Part I: Journal of Systems and Control Engineering*, vol. 230, no. 7, pp. 672–679, 2016.

[5] E. Kurvinen, C. Di, I. Petrov, J. Nerg, O. Liukkonen, R. P. Jastrzebski, D. Kepsu, P. Jaatinen, L. Aarniovuori, E. Sikanen *et al.*, "Design and manufacturing of a modular low-voltage multi-megawatt high-speed solid-rotor induction motor," *IEEE Transactions on Industry Applications*, vol. 57, no. 6, pp. 6903–6912, 2021.

[6] R. P. Jastrzebski, A. Putkonen, E. Kurvinen, and O. Pyrhönen, "Design and modeling of 2 MW AMB rotor with three radial bearing-sensor planes," *IEEE Transactions on Industry Applications*, vol. 57, no. 6, pp. 6892–6902, 2021.

[7] R. S. Srinivas, R. Tiwari, and C. Kannababu, "Application of active magnetic bearings in flexible rotordynamic systems–a state-of-the-art review," *Mechanical Systems and Signal Processing*, vol. 106, pp. 537–572, 2018.

[8] E. Kurvinen, T. Choudhury, J. Narsakka, I. Martikainen, J. Sopanen, and R. P. Jastrzebski, "Design space method for conceptual design exploration of high speed slitted solid induction motor," in *2021 IEEE International Electric Machines & Drives Conference (IEMDC)*. IEEE, 2021, pp. 1–8.

[9] R. R. Moghaddam, "High speed operation of electrical machines, a review on technology, benefits and challenges," in *2014 IEEE Energy Conversion Congress and Exposition (ECCE)*. IEEE, 2014, pp. 5539–5546.

[10] F. Zhang, G. Du, T. Wang, F. Wang, W. Cao, and J. L. Kirtley, "Electromagnetic design and loss calculations of a 1.12-mw high-speed permanent-magnet motor for compressor applications," *IEEE Transactions on Energy Conversion*, vol. 31, no. 1, pp. 132–140, 2015.

[11] A. Smirnov, N. Uzhegov, T. Sillanpää, J. Pyrhönen, and O. Pyrhönen, "High-speed electrical machine with active magnetic bearing system optimization," *IEEE Transactions on Industrial Electronics*, vol. 64, no. 12, pp. 9876–9885, 2017.

[12] K.-C. Lee, D.-K. Hong, Y.-H. Jeong, C.-Y. Kim, and M.-C. Lee, "Dynamic simulation of radial active magnetic bearing system for high speed rotor using adams and matlab co-simulation," in *2012 IEEE International Conference on Automation Science and Engineering (CASE)*, 2012, pp. 880–885.

[13] G. Pahl and W. Beitz, *Engineering Design: A Systematic Approach*, 3rd ed. Springer Verlag, United Kingdom, 2007.

[14] R. D. Cook *et al.*, *Concepts and applications of finite element analysis*. John wiley & sons, 2007.

[15] H. Cloud, G. Li, L. E. Barrett, W. C. Foiles, and E. H. Maslen, "Practical applications of singular value decomposition in rotordynamics," *Australian Journal of Mechanical Engineering*, vol. 2, no. 1, pp. 21–32, 2005.

VI. APPENDIX

Calculation algorithm

Calculation points ω_1, ω_2, ..., ω_n
for ω_i is 1 to ω_n frequency range
$\mathbf{K} = \mathbf{C} / (\omega_i \cdot \mathrm{I} - \mathbf{A})^{-1}$
$\mathbf{G}_{zu} = \mathbf{D}_u + \mathbf{K} \cdot \mathbf{B}_u$
$\mathbf{G}_{zw} = \mathbf{D}_w + \mathbf{K} \cdot \mathbf{B}_w$
$\mathbf{G}_p = (I - (\mathbf{G}_{zu}' \cdot \mathbf{G}_{zu}^{-1}) \cdot \mathbf{G}_{zu}') \cdot \mathbf{G}_{zw}$
$p = |\mathbf{G}_p|_{max}$
$f_m(i) = 1 / p$
end

VII. BIOGRAPHIES

Emil Kurvinen was born in 1988. He received M. Sc. (Tech.) and D. Sc. (Tech.) degrees in mechanical engineering from Lappeenranta University of Technology (LUT) in 2012 and 2016, respectively. In 2014-2015 he visited The University of Virginia as a Fulbright visiting scholar researching active magnetic bearings. From 2016 to 2017 he served as an engineer, in structural dynamics in FS Dynamics Finland Ltd. From 2017 to 2021 he was a postdoctoral researcher at LUT. Currently, he is a Machine Design professor at the University of Oulu. He has a solid background in machine design, especially in the design, simulation, and analysis of rotating machines. His research interests are rotating machines, especially high-speed machines, digital twins, and the integration of industrial engineering and management to technology.

Juuso Narsakka was born in Rautjärvi, Finland, in 1989. He received B. Sc. (Tech.) degrees in mechanical engineering from Lappeenranta University of Technology (LUT) in 2020, where he is currently pursuing the M. Sc. degree in mechatronic system design. His research interests are in the design of high-speed rotating machines where is needed combination of an understanding of machine dynamics and strength of materials. His work history includes jobs in industry, entrepreneurship, and teaching in LUT University.

Rafal Piotr Jastrzebski Rafal Piotr Jastrzebski (Member, IEEE) received the M.Sc. degree in electrical engineering from the Technical University of Lodz, Poland, in 2002, and the D.Sc. degree in electrical engineering from the Lappeenranta University of Technology (LUT), Finland, in 2007. At LUT, he is currently an Adjunct Professor. His research interests include design, modeling, and control of electric machines, sensors, and power electronics. He has long experience in digital control, system engineering of energy applications, mechatronic systems, active magnetic bearings, magnetic levitation systems, and bearingless machines. From 2013 to 2018, he was an Academy Research Fellow. From 2009 to 2011, he was a recipient and served as an Academy of Finland Postdoctoral Researcher.

Tuhin Choudhury was born in Seppa, India, in 1989. He received the B.Sc. (tech) degree in mechanical engineering from Sikkim Manipal University, India, in 2011, and the M.Sc. degree in mechatronic system design from LUT University, Lappeenranta, Finland, in 2018, where he is currently pursuing the Ph.D. degree with the Department of Mechanical Engineering. He was a design engineer on the development of medical devices and diagnostic instruments, from 2011 to 2016. His research interests include designing, modeling, and simulation of rotating machines, and the analysis of rotor behavior to understand the root cause of unwanted vibrations, specifically due to unbalance.

Jussi Sopanen (Member, IEEE) was born in Enonkoski, Finland, in 1974. He received the M.Sc. degree in mechanical engineering and the D.Sc. (technology) degree from LUT University, Lappeenranta, Finland, in 1999 and 2004, respectively. He was a Researcher with the Department of Mechanical Engineering, LUT University, from 1999 to 2006. He was a Product Development Engineer of electric machine manufacturing with Rotatek Finland Ltd. from 2004 to 2005. From 2006 to 2012, he was a Principal Lecturer in mechanical engineering and the Research Manager of the Faculty of Technology, Saimaa University of Applied Sciences, Lappeenranta. He is currently serving as a Professor with the Machine Dynamics Laboratory, LUT University. His research interests include rotor dynamics, multibody dynamics, and the mechanical design of electrical machines.